End-binding proteins sensitize microtubules to the action of microtubule-targeting agents

Renu Mohan[a], Eugene A. Katrukha[a], Harinath Doodhi[a], Ihor Smal[b], Erik Meijering[b], Lukas C. Kapitein[a], Michel O. Steinmetz[c], and Anna Akhmanova[a,1]

[a]Cell Biology, Faculty of Science, Utrecht University, 3584 CH, Utrecht, The Netherlands; [b]Biomedical Imaging Group Rotterdam, Department of Medical Informatics and Radiology, Erasmus Medical Center, 3000 CA, Rotterdam, The Netherlands; and [c]Biomolecular Research, Structural Biology, Paul Scherrer Insititut, CH-5232 Villigen PSI, Switzerland

Edited by J. Richard McIntosh, University of Colorado, Boulder, CO, and approved April 19, 2013 (received for review January 8, 2013)

Microtubule-targeting agents (MTAs) are widely used for treatment of cancer and other diseases, and a detailed understanding of the mechanism of their action is important for the development of improved microtubule-directed therapies. Although there is a large body of data on the interactions of different MTAs with purified tubulin and microtubules, much less is known about how the effects of MTAs are modulated by microtubule-associated proteins. Among the regulatory factors with a potential to have a strong impact on MTA activity are the microtubule plus end-tracking proteins, which control multiple aspects of microtubule dynamic instability. Here, we reconstituted microtubule dynamics in vitro to investigate the influence of end-binding proteins (EBs), the core components of the microtubule plus end-tracking protein machinery, on the effects that MTAs exert on microtubule plus-end growth. We found that EBs promote microtubule catastrophe induction in the presence of all MTAs tested. Analysis of microtubule growth times supported the view that catastrophes are microtubule age dependent. This analysis indicated that MTAs affect microtubule aging in multiple ways: destabilizing MTAs, such as colchicine and vinblastine, accelerate aging in an EB-dependent manner, whereas stabilizing MTAs, such as paclitaxel and peloruside A, induce not only catastrophes but also rescues and can reverse the aging process.

EB1 | EB3

Microtubule-targeting agents (MTAs) are a broad group of natural compounds and synthetic drugs that can promote assembly or disassembly of microtubules (MTs) at high concentrations and alter MT dynamics without significantly changing MT polymer mass at low concentrations (1, 2). These drugs are extensively used for the treatment of various cancers, and their effectiveness is mostly attributed to the ability to inhibit mitosis and disrupt tumor vasculature (1, 3, 4). Certain MTAs might also be candidates for treatment of other disorders, including neurodegenerative diseases (5).

The wide use of MTAs and the continuous search for more efficacious and less toxic agents necessitates a detailed understanding of the mechanisms of their action. Biochemical and structural studies have revealed the major binding sites for MTAs on tubulin, including the vinca, colchicine, and taxane sites (1, 3, 6). At high concentrations, MTAs binding to the vinca and colchicine site destabilize MTs and decrease the polymer mass, and will here be referred to as MT-destabilizing drugs. Taxane site-binding MTAs, such as paclitaxel, as well as some other drugs including peloruside A, promote MT stability and increase polymer mass, and will be referred to as MT-stabilizing drugs.

In vitro studies with purified tubulin have indicated that at low concentrations some MTAs specifically interact with MT ends (1). Growing MT plus ends contain a stabilizing cap of GTP-bound tubulin; when this cap is lost, MTs switch to depolymerization, a transition termed catastrophe. Detailed analysis of MT growth parameters has shown that catastrophes depend on MT age and are likely to occur after multiple intermediate steps (7–9). Certain MT-destabilizing proteins were found to either increase the rate of MT aging or lower the number of steps required for catastrophe induction (7). In this context, MT-destabilizing drugs could potentially act by similar mechanisms.

MT plus ends serve as sites of accumulation of a diverse group of factors known as MT plus end-tracking proteins (+TIPs), which control different aspects of MT dynamics and function (10–12). The core components of the +TIP network are the members of the end-binding (EB) family, highly abundant and ubiquitously expressed proteins that autonomously recognize the stabilizing cap at growing MT ends (13, 14). Since EB proteins strongly decorate freshly polymerized MT plus ends and affect MT dynamics (14–16), they might alter the effect of MTAs on MTs. In this study, we set out to investigate how the effects of MTAs on MT plus-end dynamics are modulated by the EBs.

Results

EBs Promote Catastrophe Induction by MT-Destabilizing MTAs. To examine the effect of different MTAs on MT polymerization, we used an in vitro MT assembly assay in which MTs are grown from guanylyl (α,β)methylenediphosphonate (GMPCPP)-stabilized MT seeds immobilized on coverslips (13, 17) (Fig. S1 *A–C*). MT growth was initiated by the addition of a 15 μM mixture of unlabeled and rhodamine-conjugated tubulin (at a ratio 30:1) and observed by total internal reflection fluorescence (TIRF) microscopy within ∼30 min after tubulin addition. In these conditions, the formation of polymer mass is not sufficient to cause a significant change in the concentration of soluble tubulin, making this assay optimal for observing direct effects of different agents on MT plus-end dynamics. We examined how MT polymerization is affected by MT-destabilizing drugs, including the colchicine site-binding compounds colchicine, combretastatin A4, and podophyllotoxin, and the vinca site-binding drugs vinblasine, vincristine, vinorelbine, and dolastatin 15. We found that all these MTAs could prevent sustained MT elongation in the presence of tubulin alone (Fig. 1 *A* and *B*).

To test how EBs modulate MTA activity, we next performed the same experiments in the presence of 10 nM GFP-tagged EB3. As readout, we used either rhodamine-labeled tubulin, as described above, or GFP-EB3 in the absence of fluorescent tubulin. Similar MT dynamics parameters were obtained in both conditions (Table S1), indicating that they are not affected by the use of different fluorescent markers. In agreement with our previous observations, the addition of 10 nM EB3 elevated both the MT growth rate and the catastrophe frequency by a factor of ∼1.5 (Table S1) (16). Next, we added destabilizing MTAs to the assay and found that the concentration of the drugs sufficient to inhibit sustained MT

Author contributions: R.M. and A.A. designed research; R.M. and H.D. performed research; I.S. and E.M. contributed new reagents/analytic tools; R.M., E.A.K., H.D., L.C.K., M.O.S., and A.A. analyzed data; and R.M., E.A.K., L.C.K., M.O.S., and A.A. wrote the paper.

The authors declare no conflict of interest.

This article is a PNAS Direct Submission.

[1]To whom correspondence should be addressed. E-mail: a.akhmanova@uu.nl.

This article contains supporting information online at www.pnas.org/lookup/suppl/doi:10.1073/pnas.1300395110/-/DCSupplemental.

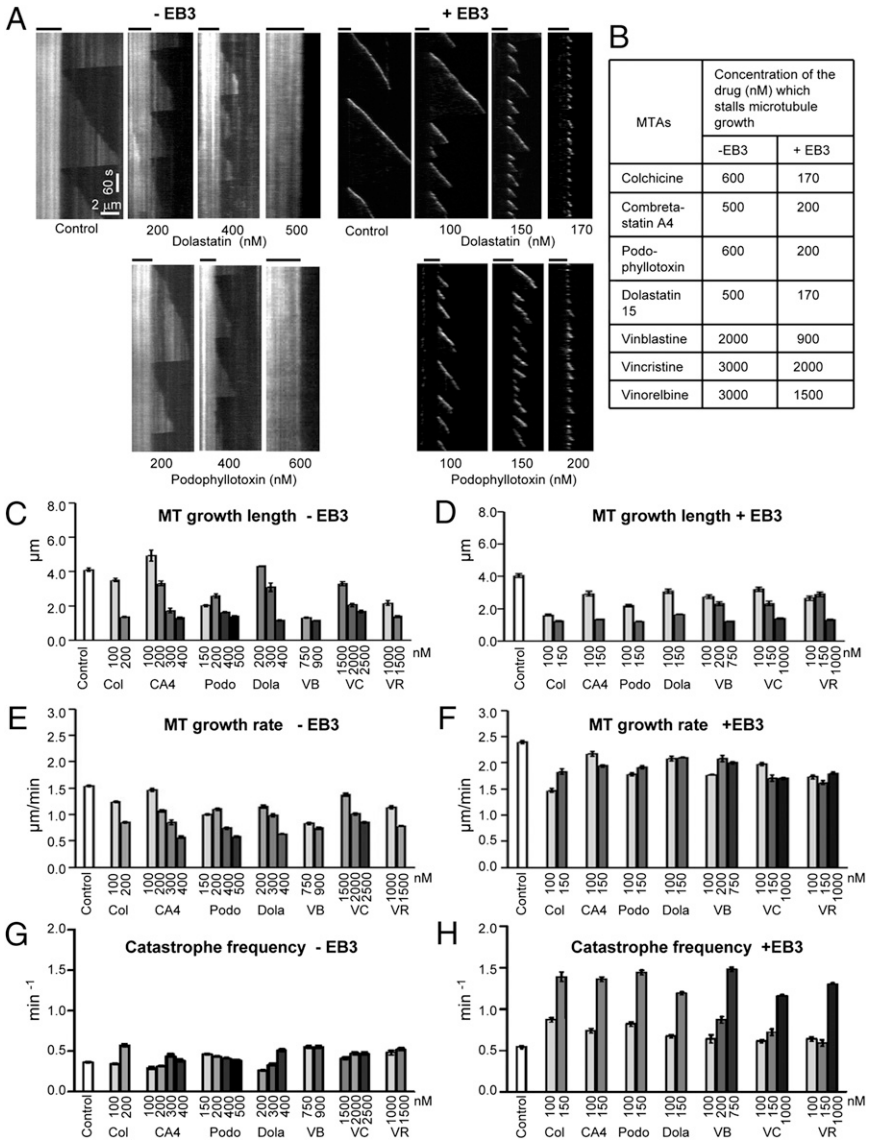

MTAs	Concentration of the drug (nM) which stalls microtubule growth	
	-EB3	+ EB3
Colchicine	600	170
Combretastatin A4	500	200
Podophyllotoxin	600	200
Dolastatin 15	500	170
Vinblastine	2000	900
Vincristine	3000	2000
Vinorelbine	3000	1500

Fig. 1. Effects of MT-destabilizing MTAs on MT dynamics. (*A*) Representative kymographs illustrating the dynamics of rhodamine-labeled MTs grown in the absence of GFP-EB3 (*Left*) or GFP-EB3 labeled MTs (*Right*) in the presence of MT-destabilizing MTAs. The positions of MT seeds are indicated by black lines above the kymographs. (*B*) MTA concentrations sufficient to inhibit MT outgrowth from the seed, so that no MT elongation exceeding 0.5 μm was observed within a 10-min period. (*C–H*) Length of MT growth episodes, MT growth rate, and catastrophe frequency at increasing concentrations of the indicated MTAs. Error bars represent SEM. Abbreviations: CA4, combretastatin A4; Col, colchicine; Dola, dolastatin 15; Podo, podophyllotoxin; VB, vinblastine; VC, vincristine; VR, vinorelbine.

elongation was by a factor of 2–3 lower when MTs were grown in the presence of EB3 (Fig. 1 *A* and *B*), indicating that EB3 sensitizes MTs to the action of MTAs.

To understand how EB3 cooperates with MTAs, we measured parameters of MT dynamics using an automated kymograph analysis algorithm, which allowed us to analyze a large number of MT growth events (17, 18). We found that, in the absence of EB3, increasing concentrations of destabilizing MTAs decreased MT elongation primarily by reducing MT growth rate (Fig. 1 *C*, *E*, and *G*), as previously shown (19–22). In contrast, the catastrophe frequency increased only mildly, if at all (Fig. 1 *C*, *E*, and *G*, and Table S2). In the presence of EB3, only a mild change in MT growth rate was observed at drug concentrations close to the ones completely inhibiting MT outgrowth (Fig. 1 *D* and *F* and Table S3); instead, we saw a dramatic increase in catastrophe frequency (Fig. 1 *A* and *H* and Table S3). When the drug concentration was further elevated, very high catastrophe frequency induced a state whereby only extremely short MT outgrowth episodes at the plus end of the GMPCPP-stabilized seed could be seen (Fig. 1*A* and Fig. S1*D*). The same effect was observed in the presence of another member of the EB family, EB1 (Fig. S2*A*). These results demonstrate that destabilizing MTAs, irrespective of their binding site, increase the catastrophe frequency of EB-bound MTs at concentrations that do not affect MTs when the EBs are absent. Thus, EBs sensitize MTs by evoking MTA-induced catastrophes.

Next, we tested whether this effect can also be observed in cells. Using live imaging of MT plus-end dynamics in HeLa cells stably expressing EB3-GFP, we observed strong catastrophe induction by nanomolar concentrations of vinblastine in conditions when the MT growth rate was only mildly reduced (Fig. 2 and Table S4). This indicates that our in vitro observations reflect a physiologically relevant phenomenon.

MT-Destabilizing MTAs Accelerate MT Aging. Previous work has shown that the catastrophe rate depends on MT age, as "younger" MTs have a lower probability to undergo a catastrophe than

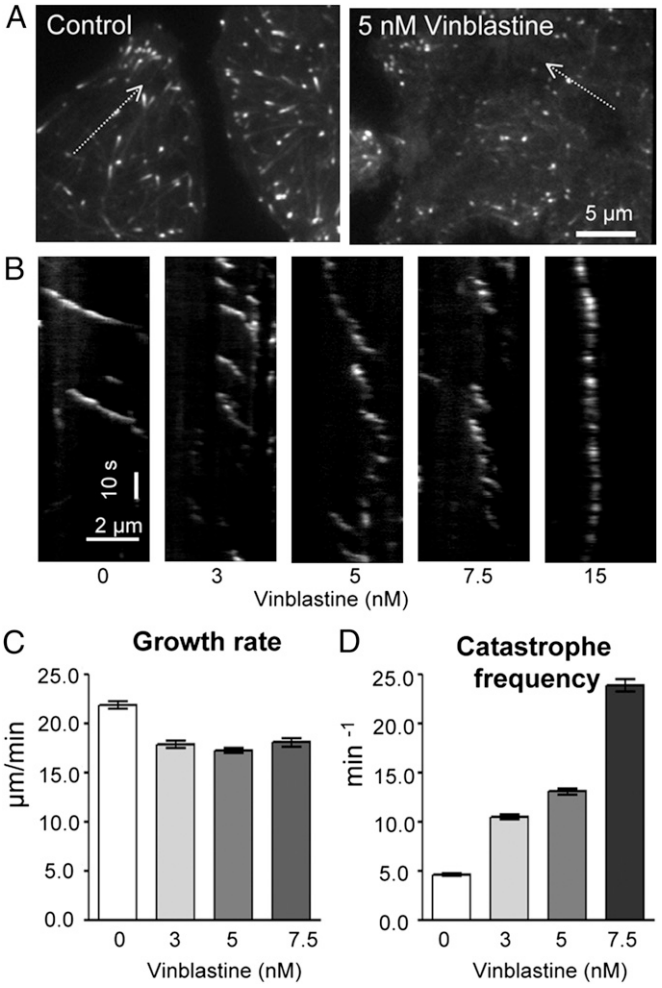

Fig. 2. Vinblastine increases MT catastrophe frequency in cells in a concentration-dependent manner. HeLa cells stably expressing EB3-GFP were treated with the indicated concentrations of vinblastine for 30 min and imaged with a 0.5-s time interval. (*A*) Live images of HeLa cells expressing EB3-GFP, either in control conditions or after 30 min of treatment with 5 nM vinblastine. Examples of MT tips used for making kymographs are indicated by arrows. (*B*) Kymographs illustrating the behavior of individual MT plus ends. (*C* and *D*) Quantifications of MT growth rate and catastrophe frequency. Error bars represent SEM.

"older" ones (7, 8). This suggests that not one but multiple intermediate catastrophe-promoting steps have to occur during MT polymerization before the transition from growth to shrinkage takes place (7, 8). To test how MTAs affect MT aging in the absence or presence of EB3, we analyzed the precise distribution of MT growth times. If catastrophes ensue after several randomly occurring steps of equal rate, durations of MT growth episodes should follow a gamma distribution described by two parameters: the minimum number of intermediate steps (n) and the rate at which these steps occur (r).

The distributions of MT growth times in our assays could indeed be fitted by gamma distributions (Fig. 3 *A* and *B*). We determined the parameters n and r for different conditions and found that they were only mildly affected by the addition of EB3 alone or by the addition of destabilizing drugs to MTs grown in the absence of EBs (Fig. 3 *C*–*F* and Table S5). The number of steps was between 3 and 4.5 in different conditions, which is comparable with the values determined previously for tubulin alone (7). In the presence of EB3, increasing concentrations of MT-destabilizing MTAs had no strong effect on the step parameter, whereas the value of the rate parameter was elevated (Fig. 3 *D* and *F*, and Table S5). Thus, EB3-bound MTs age more rapidly in the presence of MTAs.

Accumulation of EB Proteins at the MT Tips Is Affected by MT Aging. Although the mechanistic details of the catastrophe-promoting steps are unknown, one possibility is that MT lattice defects arise during polymerization and are propagated so that the MT tip structure is altered (Fig. 4*A*). Because EB proteins bind to the stabilizing cap (13, 14), EB accumulation at the MT end could potentially reflect such age-related changes. To test this hypothesis, we measured the intensity of GFP-EB3 signal at MT plus ends during MT growth and observed that, in addition to the increase during growth initiation and a steep decrease before the catastrophe, EB3 comet intensity fluctuated substantially (Fig. 4 *B* and *C*). These fluctuations could reflect the occurrence of transient MT lattice defects or other alterations in the MT tip structure, which get corrected while the MT grows. Importantly, in addition to these fluctuations, we also observed that the EB3 signal at the MT plus end gradually decreased during the growth event, which could be observed both in control conditions (relatively long growth episodes) and was even more obvious in the presence of MTAs (substantially shorter growth episodes; Fig. 4 *B*–*D*). A similar decrease in signal intensity at the MT end before the catastrophe has previously been observed in reconstitution experiments with the fission yeast homolog of EB3, Mal3 (14). The gradual decrease of the EB comet intensity at growing MT ends supports the view that catastrophe induction is a gradual multistep process.

Fewer Steps Are Needed to Cause a Catastrophe of a MT After a Rescue. A consequence of the "MT defect propagation" model is that, during MT depolymerization, the "memory" of the MT defects will be obliterated. However, if a MT is rescued, some of the propagated defects could persist (Fig. 4*A*), and fewer steps would be required to cause a new catastrophe. To test this prediction, we examined the distribution of growth times upon rescues and found that the number of steps occurring before rescued MTs underwent a catastrophe was approximately twofold lower than for MTs growing from the GMPCPP-stabilized MT seed in the same conditions (Fig. 4 *E* and *F*). This result demonstrates that rescued MTs display distinct properties with respect to catastrophe: they behave as if they are more aged than those originating from the seed.

MT-Stabilizing MTAs Promote Both Catastrophes and Rescues in the Presence of EBs. To obtain additional insights into the relationship between catastrophes and rescues, we turned to MT-stabilizing drugs, which we expected to be rescue inducers. We used paclitaxel, which binds to the taxane site, and peloruside A, which binds to a so far poorly characterized tubulin site (23). At low concentrations, the two drugs had no strong effect on the MT growth rate (Table S2). In the absence of EBs, both drugs suppressed catastrophes: no catastrophes at all could be detected in the presence of 100 nM paclitaxel and 50 nM peloruside A (Table S2). However, upon the addition of EB3, the drugs acted in the opposite way: a mild but significant increase in catastrophe frequency was observed (Fig. 4 *G* and *H* and Tables S3 and S6). These results are consistent with a previous study of the effect of paclitaxel and epothilone B on EB3-decorated MTs (24). For paclitaxel, catastrophe induction was more obvious for lower concentrations such as 100 nM than for higher concentrations (Fig. 4*H*). Thus, EB3 alters the MT growth properties in such a way that even MT-stabilizing agents promote rather than suppress catastrophes.

Despite the slightly increased catastrophe frequency in the presence of EB3, the MT-stabilizing drugs did not inhibit MT elongation because they also strongly stimulated rescues (Fig. 4 *G* and *I*). This effect was not specific to EB-bound MTs as it was also observed at 50 nM paclitaxel in the absence of EB3

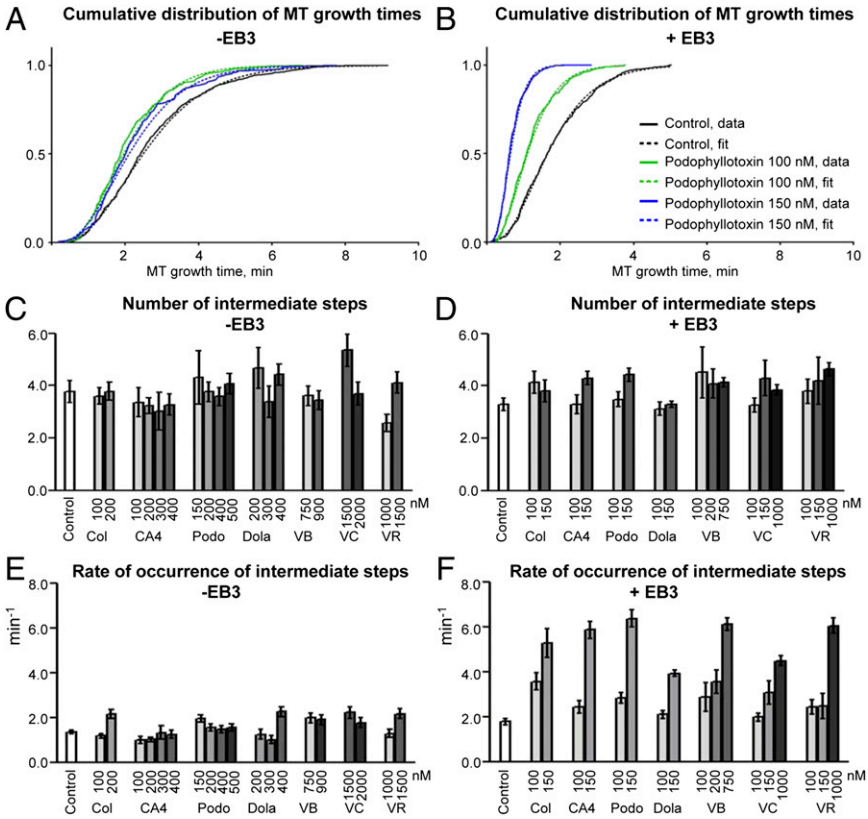

Fig. 3. Analysis of the duration of MT growth episodes. (*A* and *B*) Cumulative distributions of MT growth times (times from MT outgrowth to catastrophe) in the presence of different concentrations of podophyllotoxin with and without GFP-EB3 (solid lines). Gamma fits of the distributions are shown by stippled lines. (*C*–*F*) Gamma distribution parameters *n* (number of intermediate states) and *r* (rate of occurrence of intermediate states) in different conditions, as indicated. Abbreviations are the same as in Fig. 1*C*. Error bars indicate SEM.

(Table S2; at higher concentrations catastrophes, and hence rescues, were absent). Interestingly, in addition to randomly occurring rescues, the drugs also induced the appearance of "stable rescue points"—MT sites located at a significant distance from the seed that initiated repeated rescue events (Fig. 4*G* and Fig. S2*B*). To examine the difference between stable and random rescue points, we measured the number of steps before catastrophe (Table S7). We found that, for MTs originating from stable rescue points, this was similar to the number of steps observed for MTs growing from seeds, whereas catastrophes upon random rescue required fewer steps (Fig. 4 *E* and *F*). Thus, besides promoting random rescues, MT-stabilizing agents can introduce into the MT lattice specific sites where the consequences of the propagating MT aging process are eliminated.

Discussion

In this study, we have shown that EB proteins strongly modulate the effect of different types of MTAs on MT dynamics. In the absence of EBs, MT-destabilizing MTAs suppressed MT elongation by slowing down MT polymerization. In the presence of EBs, however, MT growth was inhibited due to strongly increased catastrophe frequency already at concentrations of destabilizing MTAs that were insufficient to substantially affect the MT growth rate. Furthermore, although MT-stabilizing drugs suppressed catastrophes of MTs grown without EBs, they mildly promoted catastrophes when EBs were added. Thus, irrespective of the nature of the binding site and their molecular mechanism of action, MTAs increase the catastrophe frequency of EB-bound MTs (Fig. 4*J*). Consistently, low levels of MT-stabilizing (24, 25) and MT-destabilizing MTAs (26, 27) (Fig. 2) have been found to promote catastrophes in cells.

Our assay is different from that used in many previous analyses of MTA effects in vitro, because we perform measurements immediately after tubulin addition, in conditions when only little MT polymer is formed, and, therefore, drug-induced changes in MT polymer mass do not substantially affect our results. Despite the experimental differences, we observed that MT growth rate was decreased by destabilizing MTAs similar to previous studies (19–22). The catastrophe rate was mildly increased or unchanged, again similar to previous studies (19), although a reduction in this parameter has also been observed in some previously described assays (20–22). MT depolymerization rate did show some variation but remained ∼10 times higher than the growth rate (Tables S2 and S3) and was not analyzed here in detail.

Reduced MT growth in the absence of EBs was likely due to the alteration of the complex kinetics of subunit addition and removal at the MT tip (28), and not tubulin sequestration by the drugs, because the MTA concentrations completely inhibiting MT outgrowth were 5–30 times lower than the tubulin concentration in the assay. In the presence of EBs, a direct effect on the MTs rather than soluble tubulin availability is even more likely, because the drug concentrations that effectively blocked MT elongation were even lower. Analysis of MT growth times showed that, in these conditions, MT-destabilizing MTAs increased the catastrophe frequency in a concentration-dependent manner by elevating the occurrence rate but not the number of intermediate catastrophe-promoting steps. This suggests that these drugs do not fundamentally alter the mechanism of MT aging but, in interplay with EBs, accelerate its progression. To understand the underlying mechanism, more insight into the nature of catastrophe-inducing steps would be needed. These steps might correspond to propagating MT lattice defects, which could be initiated by the

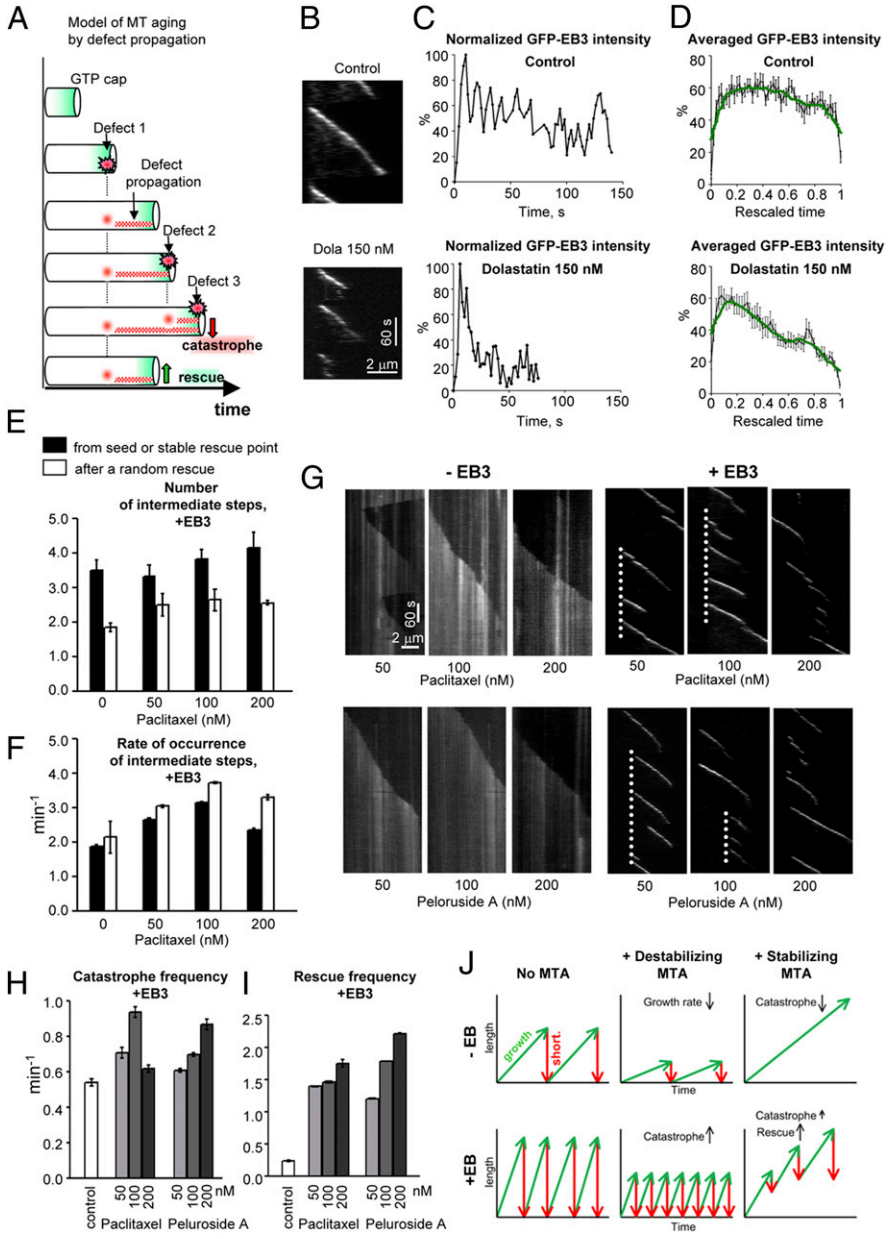

Fig. 4. Analysis of EB3 comet intensity and the effects of MT-stabilizing MTAs on MT dynamics. (*A*) Scheme illustrating the model of MT aging by propagating MT lattice defects. (*B–D*) Analysis of GFP-EB3 intensity at MT plus ends in control samples and in the presence of 150 nM dolastatin. (*B*) Representative MT growth events. (*C*) Normalized GFP-EB3 intensity profiles for the events shown in *B*. (*D*) Averaged profiles of normalized GFP-EB3 intensity ($n = 16$ for both plots) where time was rescaled so that the duration of each growth episode is equal to 1 (black lines; error bars represent SEM). To illustrate the general trend, the mean values were smoothened using a sliding window of size 10 (green lines). (*E* and *F*) Gamma distribution parameters *n* (number of intermediate states) and *r* (rate of occurrence of intermediate states) in different conditions, as indicated. Catastrophe times were calculated separately for MT growth events originating from the seed or a stable rescue point in the presence of paclitaxel, and after a random MT rescue. Stable rescue points were defined as MT lattice sites where multiple rescues (more than three) occurred. Error bars represent SEM. (*G*) Representative kymographs illustrating MT dynamics in the absence (*Left*) or presence of GFP-EB3 (*Right*) and MT-stabilizing MTAs. The stippled white lines indicate the positions of stable rescue points. (*H* and *I*) MT catastrophe and rescue frequency as a function of concentration of the indicated MTAs. Error bars indicate SEM. (*J*) Schematic summary of the effects of MTAs on MT dynamics in the absence and presence of GFP-EB3.

incorporation of a curved tubulin dimer in the presence of colchicine (29) or a kink at the interdimer interface in the presence of vinca alkaloids (30). EBs could potentially promote incorporation or propagation of these defects by, for example, affecting interprotofilament contacts or by altering the rate of GTP hydrolysis in the stabilizing cap (31).

MT-stabilizing drugs increased both the catastrophe and the rescue rates in the presence of EB (Fig. 4*J*). These drugs could also enhance the formation or propagation of MT lattice defects in the presence of EBs, for example, by altering the structure of MT protofilaments (32). However, their effect on catastrophes was much milder. In the presence of paclitaxel, the catastrophe rate was increased by ~70% at 100 nM, but only by ~10% at higher concentrations. This is likely due to the ability of this drug to stabilize lateral contacts between tubulin subunits across protofilaments (2, 33) and to stimulate rescues, thus counteracting the catastrophe induction. The complex effect of paclitaxel on MT dynamics is consistent with previous studies that

reported concentration dependent effects on MT dynamics parameters (34–36). An interesting property of stabilizing MTAs that we observed is their ability to induce stable rescue points, which might arise when several stabilizing contacts in the MT lattice form close to each other. Analysis of the number of catastrophe-inducing steps indicated that stable rescue points behave similar to MT seeds, suggesting that these sites could block the propagation of defects in aging MTs.

Given that EB proteins are highly abundant and ubiquitous, the synergy between MTAs and EBs in catastrophe induction has important consequences for the effects that MTAs exert in cells. During cell division, a high catastrophe frequency will affect the organization of the mitotic apparatus, MT attachment to kinetochores and the spindle assembly checkpoint (37). In interphase, increased catastrophes will cause less efficient penetration of MTs into lamellae or the actin-rich cortex at cell–cell junctions, leading to altered cell migration and adhesion (38, 39). Notably, these MT-based effects are important for cancer cell physiology. Our findings may thus be relevant for the development and improvement of novel generation of MTAs.

Materials and Methods

Stock solutions of combretastatin A4, podophyllotoxin, dolastatin 15 (Sigma), paclitaxel (Enzo Life Sciences), vincristine (a gift from S. Honore, Centre National de la Recherche Scientifique, Marseille, France) and peloruside A (a gift from F. Díaz, Consejo Superior de Investigaciones Cientificas, Madrid, Spain) were prepared in DMSO, whereas colchicine, vinblastine sulfate salt, and vinorelbine ditartrate salt (Sigma) were dissolved in distilled water. All of the drugs were further diluted in the assay buffer (80 mM Pipes, 4 mM $MgCl_2$, 1 mM EGTA, pH adjusted to 6.8 with KOH).

Reconstitution of plus-end tracking in vitro was performed as described previously (17) (see *SI Materials and Methods* for details). MTs labeled with either 0.5 μM rhodamine-conjugated tubulin or 10 nM GFP-EB3 were imaged using a TIRF microscope at 2 s per frame with 100-ms exposure time. Imaging was performed within the first 35 min after tubulin addition.

HeLa cells stably expressing EB3-GFP were treated with different drug concentrations and imaged 30 min after drug addition. The TIRF microscope was used in a semi-TIRF mode, which allowed optimal visualization of the ~0.5- to 1-μm-thick part of the cell proximal to the coverslip.

Maximum-intensity projections and kymographs were made using Metamorph. MT dynamics parameters were determined from kymographs using an optimized version of the custom-made JAVA plug in for ImageJ described previously (17). The gamma distribution parameters were estimated by the fitting of experimental cumulative distributions of growth times as described (7). For details of quantifications and statistical analysis, see *SI Materials and Methods*.

ACKNOWLEDGMENTS. We thank K. Bargsten for the preparation of EB protein samples, S. Honore and F. Díaz for the gift of reagents, and M. Dogterom and members of her laboratory for critical comments on our manuscript. This work was supported by a European Molecular Biology Organization Long-Term Fellowship and Marie Curie International Incoming Fellowship (to R.M.), by a Human Frontier Science Program grant, by a Netherlands Organization for Scientific Research Aard-en Levenswetenschapen VICI grant (to A.A.), and by Swiss National Science Foundation Grant 310030B_138659 and Swiss SystemsX.ch Initiative Grant BIP-2011/122 (to M.O.S.).

1. Jordan MA, Wilson L (2004) Microtubules as a target for anticancer drugs. *Nat Rev Cancer* 4(4):253–265.
2. Amos LA (2011) What tubulin drugs tell us about microtubule structure and dynamics. *Semin Cell Dev Biol* 22(9):916–926.
3. Stanton RA, Gernert KM, Nettles JH, Aneja R (2011) Drugs that target dynamic microtubules: A new molecular perspective. *Med Res Rev* 31(3):443–481.
4. Zhou J, Giannakakou P (2005) Targeting microtubules for cancer chemotherapy. *Curr Med Chem Anticancer Agents* 5(1):65–71.
5. Ballatore C, et al. (2012) Microtubule stabilizing agents as potential treatment for Alzheimer's disease and related neurodegenerative tauopathies. *J Med Chem* 55(21): 8979–8996.
6. Calligaris D, et al. (2010) Microtubule targeting agents: From biophysics to proteomics. *Cell Mol Life Sci* 67(7):1089–1104.
7. Gardner MK, Zanic M, Gell C, Bormuth V, Howard J (2011) The depolymerizing kinesins Kip3 (kinesin-8) and MCAK (kinesin-13) are catastrophe factors that destabilize microtubules by different mechanisms. *Cell* 147(5):1092–1103.
8. Odde DJ, Cassimeris L, Buettner HM (1995) Kinetics of microtubule catastrophe assessed by probabilistic analysis. *Biophys J* 69(3):796–802.
9. Gardner MK, Zanic M, Howard J (2013) Microtubule catastrophe and rescue. *Curr Opin Cell Biol* 25(1):14–22.
10. Akhmanova A, Steinmetz MO (2008) Tracking the ends: A dynamic protein network controls the fate of microtubule tips. *Nat Rev Mol Cell Biol* 9(4):309–322.
11. Howard J, Hyman AA (2003) Dynamics and mechanics of the microtubule plus end. *Nature* 422(6933):753–758.
12. Kumar P, Wittmann T (2012) +TIPs: SxIPping along microtubule ends. *Trends Cell Biol* 22(8):418–428.
13. Bieling P, et al. (2007) Reconstitution of a microtubule plus-end tracking system in vitro. *Nature* 450(7172):1100–1105.
14. Maurer SP, Fourniol FJ, Bohner G, Moores CA, Surrey T (2012) EBs recognize a nucleotide-dependent structural cap at growing microtubule ends. *Cell* 149(2):371–382.
15. Seetapun D, Castle BT, McIntyre AJ, Tran PT, Odde DJ (2012) Estimating the microtubule GTP cap size in vivo. *Curr Biol* 22(18):1681–1687.
16. Komarova Y, et al. (2009) Mammalian end binding proteins control persistent microtubule growth. *J Cell Biol* 184(5):691–706.
17. Montenegro Gouveia S, et al. (2010) In vitro reconstitution of the functional interplay between MCAK and EB3 at microtubule plus ends. *Curr Biol* 20(19):1717–1722.
18. Smal I, Grigoriev I, Akhmanova A, Niessen WJ, Meijering E (2009) Accurate estimation of microtubule dynamics using kymographs and variable-rate particle filters. *Conf Proc IEEE Eng Med Biol Soc* 2009:1012–1015.
19. Ngan VK, et al. (2000) Novel actions of the antitumor drugs vinflunine and vinorelbine on microtubules. *Cancer Res* 60(18):5045–5051.
20. Panda D, Jordan MA, Chu KC, Wilson L (1996) Differential effects of vinblastine on polymerization and dynamics at opposite microtubule ends. *J Biol Chem* 271(47): 29807–29812.
21. Toso RJ, Jordan MA, Farrell KW, Matsumoto B, Wilson L (1993) Kinetic stabilization of microtubule dynamic instability in vitro by vinblastine. *Biochemistry* 32(5):1285–1293.
22. Panda D, Daijo JE, Jordan MA, Wilson L (1995) Kinetic stabilization of microtubule dynamics at steady state in vitro by substoichiometric concentrations of tubulin-colchicine complex. *Biochemistry* 34(31):9921–9929.
23. Huzil JT, et al. (2008) A unique mode of microtubule stabilization induced by peloruside A. *J Mol Biol* 378(5):1016–1030.
24. Pagano A, et al. (2012) Epothilone B inhibits migration of glioblastoma cells by inducing microtubule catastrophes and affecting EB1 accumulation at microtubule plus ends. *Biochem Pharmacol* 84(4):432–443.
25. Chan A, Andreae PM, Northcote PT, Miller JH (2011) Peloruside A inhibits microtubule dynamics in a breast cancer cell line MCF7. *Invest New Drugs* 29(4):615–626.
26. Yenjerla M, Cox C, Wilson L, Jordan MA (2009) Carbendazim inhibits cancer cell proliferation by suppressing microtubule dynamics. *J Pharmacol Exp Ther* 328(2): 390–398.
27. Pourroy B, et al. (2006) Antiangiogenic concentrations of vinflunine increase the interphase microtubule dynamics and decrease the motility of endothelial cells. *Cancer Res* 66(6):3256–3263.
28. Gardner MK, et al. (2011) Rapid microtubule self-assembly kinetics. *Cell* 146(4): 582–592.
29. Dorléans A, et al. (2009) Variations in the colchicine-binding domain provide insight into the structural switch of tubulin. *Proc Natl Acad Sci USA* 106(33):13775–13779.
30. Gigant B, et al. (2005) Structural basis for the regulation of tubulin by vinblastine. *Nature* 435(7041):519–522.
31. Maurer SP, Bieling P, Cope J, Hoenger A, Surrey T (2011) GTPgammaS microtubules mimic the growing microtubule end structure recognised by end-binding proteins (EBs). *Proc Natl Acad Sci USA* 108(10):3988–3993.
32. Elie-Caille C, et al. (2007) Straight GDP-tubulin protofilaments form in the presence of taxol. *Curr Biol* 17(20):1765–1770.
33. Prota AE, et al. (2013) Molecular mechanism of action of microtubule-stabilizing anticancer agents. *Science* 339(6119):587–590.
34. Derry WB, Wilson L, Jordan MA (1998) Low potency of taxol at microtubule minus ends: Implications for its antimitotic and therapeutic mechanism. *Cancer Res* 58(6): 1177–1184.
35. Jordan MA, Toso RJ, Thrower D, Wilson L (1993) Mechanism of mitotic block and inhibition of cell proliferation by taxol at low concentrations. *Proc Natl Acad Sci USA* 90(20):9552–9556.
36. Derry WB, Wilson L, Jordan MA (1995) Substoichiometric binding of taxol suppresses microtubule dynamics. *Biochemistry* 34(7):2203–2211.
37. Bakhoum SF, Compton DA (2012) Kinetochores and disease: Keeping microtubule dynamics in check!. *Curr Opin Cell Biol* 24(1):64–70.
38. Brieher WM, Yap AS (2013) Cadherin junctions and their cytoskeleton(s). *Curr Opin Cell Biol* 25(1):39–46.
39. Stehbens S, Wittmann T (2012) Targeting and transport: How microtubules control focal adhesion dynamics. *J Cell Biol* 198(4):481–489.